CORRELATIONS AND DISTINGUISHABILITY CHALLENGES IN SUPERNOVA MODELS:
INSIGHTS FROM FUTURE NEUTRINO DETECTOR

Maria Manuela Saez[1,2], Ermal Rrapaj[1,2,3], Akira Harada[1], Shigehiro Nagataki[1,4,5], Yong Qian[6]

1. Riken iTHEMS
2. Department of Physics, UC Berkeley
3. Lawrence Berkeley National Laboratory
4. ABBL, RIKEN Cluster for Pioneering Research
5. ABBG , Okinawa Institute of Science and Technology Graduate University
6. University of Minnesota, Minneapolis, Minnesota

Joint RIKEN/N3AS Workshop on Multi-Messenger Astrophysics

Core-Collapse Supernovae

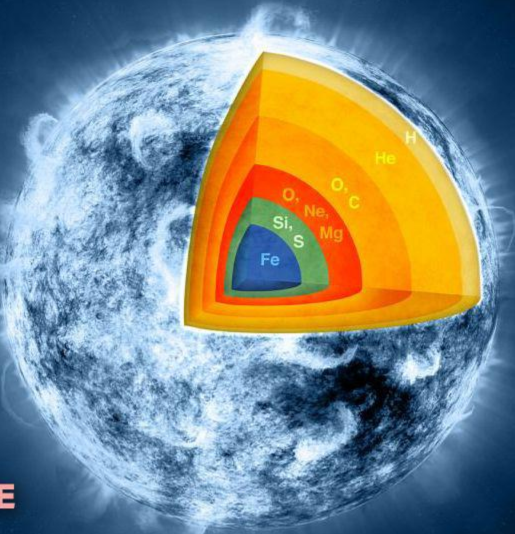

1. Core increases T without degenerating: Hydrodynamic burning of H, He, O, C, Ne, Si. Layers with material from a different burning stage.

2. Silicon burning shell: core reaches Chandrasekhar mass, and the material degenerates.

3. "Pre-supernova" stage: T ~ 10^{10}K and rho ~ 10^{10}g/cm3

4. Pressure of the degenerate electrons can no longer stabilize the core → **COLLAPSE**

5. Mechanisms that accelerate the collapse:

$$^{56}\mathrm{Fe} + \gamma \rightarrow 13^4\mathrm{He} + 4\mathrm{n} \qquad (A, Z) + e^- \rightarrow (A, Z-1) + \nu_e$$

6. Neutrino trapping and the nuclear saturation density is reached: STOPS THE IMPLOSION, Interactions begin to be repulsive → **EXPLOSION**

7. Collision between the outer layer that continue falling to the center with the inner core → **SHOCK WAVE**

8. Neutrinos of all flavors are produced

$$e^- + e^+ \rightarrow \nu_e + \bar{\nu}_e \qquad N + N \rightarrow N + N + \nu + \bar{\nu}$$

$$\nu_e + \bar{\nu}_e \rightarrow \nu_x + \bar{\nu}_x \qquad e^- + p \rightarrow n + \nu_e$$

INITIAL FLUXES

QKE

NEUTRINO OSCILLATION
MODELLING

FLUXES THAT REACH THE EARTH

INITIAL FLUXES

The initial spectral distribution is often parametrized by a parameter-fit that allows for deviations from a strictly thermal spectrum.

SUPERNOVA SIMULATIONS PROVIDE THE INDICATIVE VALUES OF THE PARAMETERS

(EoS?, unsuccessful explosions, different approx, etc.)

QKE

NEUTRINO OSCILLATION MODELLING

→

FLUXES THAT REACH THE EARTH

INITIAL FLUXES

The initial spectral distribution is often parametrized by a parameter-fit that allows for deviations from a strictly thermal spectrum.

SUPERNOVA SIMULATIONS PROVIDE THE INDICATIVE VALUES OF THE PARAMETERS

(EoS?, unsuccessful explosions, different approx, etc.)

QKE

NEUTRINO OSCILLATION MODELLING

NEUTRINO MASS ORDERING PROBLEM

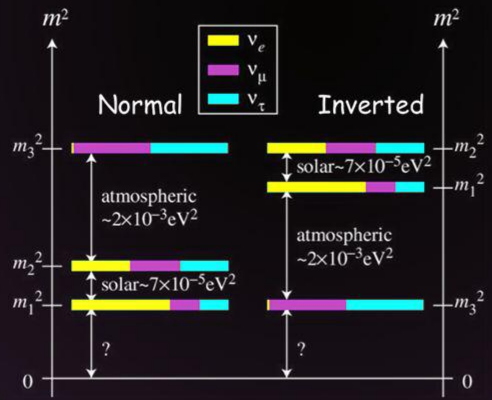

FLUXES THAT REACH THE EARTH

INITIAL FLUXES

The initial spectral distribution is often parametrized by a parameter-fit that allows for deviations from a strictly thermal spectrum.

SUPERNOVA SIMULATIONS PROVIDE THE INDICATIVE VALUES OF THE PARAMETERS

(EoS?, unsuccessful explosions, different approx, etc.)

QKE

NEUTRINO OSCILLATION MODELLING

NEUTRINO MASS ORDERING PROBLEM

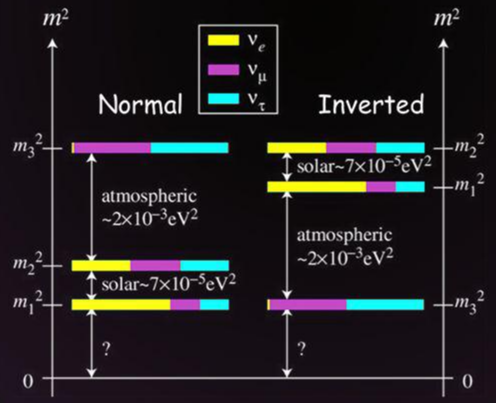

FLUXES THAT REACH THE EARTH

DETECTOR CHARACTERISTICS

DETECTION CHANNEL

RELEVANT CROSS-SECTIONS

UPCOMING GALACTIC SUPERNOVA:
OPPORTUNITY TO COMPARE MODEL PREDICTIONS WITH OBSERVATIONS.

- **Current research heavily relies on computer simulations.**
- **Research groups worldwide conduct SN simulations**
  → different dimensionalities, progenitor masses , compositions, rotational velocities, EoS, approximations.
- **Vary in complexity:**

Highly detailed models:
→ Substantial computational resources.
→ Simulate individual or few progenitors accurately
Simplified studies:
→ Spherical symmetry
→ Approximations in neutrino transport
→ Reduced computational demands
→ Less realistic but allows large number of simulations

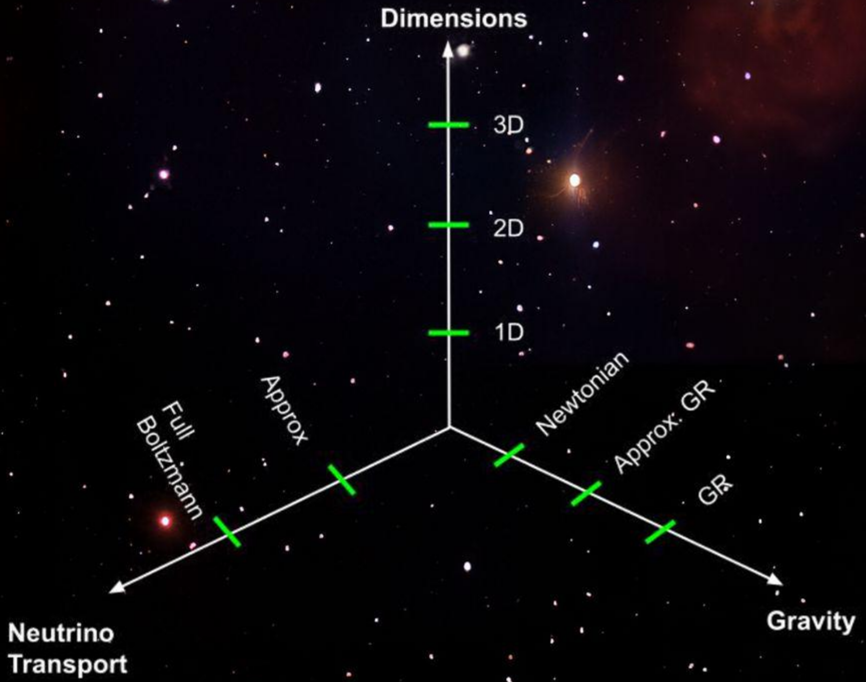

Goal

- Conduct a comprehensive analysis of the expected neutrino signal in three future neutrino detectors for a large number of initial SN models incorporating simulations from various groups.
- Expected neutrino signal derived from Boltzmann-radiation-hydrodynamics models studied for the very first time.
- Examine correlation and patterns in signals.
- Assess the potential of planned neutrino detectors in discriminating between different SN models.

SN Fluxes at the Earth

$$F^0_{\nu_\alpha} = \frac{L_{\nu_\alpha}(t)}{4\pi d^2 \langle E_{\nu_\alpha}(t)\rangle} f_{\nu_\alpha}(E_{\nu_\alpha}, t)$$

Un-oscillated fluxes

$$f_{\nu_\alpha}(E_\nu, t) = \mathcal{N}\left(\frac{E_\nu}{\langle E_{\nu_\alpha}(t)\rangle}\right)^{\beta_{\nu_\alpha}(t)} \exp\left[-(\beta_{\nu_\alpha}(t)+1)\frac{E_\nu}{\langle E_{\nu_\alpha}(t)\rangle}\right] \qquad \frac{\langle E^2_{\nu_\alpha}\rangle}{\langle E_{\nu_\alpha}\rangle^2} = \frac{2+\beta_{\nu_\alpha}}{1+\beta_{\nu_\alpha}}.$$

Normalized distribution

$$\begin{aligned} F_{\nu_e} &= P_e F^0_{\nu_e} + (1-P_e)F^0_{\nu_x} \ , \\ F_{\bar{\nu}_e} &= \bar{P}_e F^0_{\bar{\nu}_e} + (1-\bar{P}_e)F^0_{\bar{\nu}_x} \ , \\ F_{\nu_x} &= \frac{1}{2}(1-P_e)F^0_{\nu_e} + \frac{1}{2}(1+P_e)F^0_{\nu_x} \ , \\ F_{\bar{\nu}_x} &= \frac{1}{2}(1-\bar{P}_e)F^0_{\bar{\nu}_e} + \frac{1}{2}(1+\bar{P}_e)F^0_{\bar{\nu}_x} \ . \end{aligned}$$

Neutrino fluxes at Earth (MSW)

NMO →

$$\begin{aligned} P_e &= |U_{e1}|^2 P_H P_L + |U_{e2}|^2 P_H (1-P_L) + |U_{e3}|^2 (1-P_H) \ , \\ \bar{P}_e &= |U_{e1}|^2 \ , \end{aligned}$$

IMO →

$$\begin{aligned} P_e &= |U_{e1}|^2 P_L + |U_{e2}|^2 (1-P_L) \ , \\ \bar{P}_e &= |U_{e1}|^2 \bar{P}_H + |U_{e3}|^2 (1-\bar{P}_H) \ , \end{aligned}$$

Expected signal in underground detectors

$$\frac{dN(t)}{dt} = N_{tar} \int_{E_{th_d}}^{E_{max}} dE \int_{E_{th_r}}^{\infty} dE_\nu \int_0^{\infty} dE' \epsilon(E') \frac{dF_\nu}{dE_\nu}(E_\nu, t) \frac{d\sigma}{dE'}(E_\nu, E') G(E, E', \delta),$$

Expected signal in underground detectors

$$\frac{dN(t)}{dt} = N_{tar} \int_{E_{th_d}}^{E_{max}} dE \int_{E_{th_r}}^{\infty} dE_\nu \int_0^{\infty} dE' \epsilon(E') \frac{dF_\nu}{dE_\nu}(E_\nu, t) \frac{d\sigma}{dE'}(E_\nu, E') G(E, E', \delta),$$

Detector info Thresholds, Fiducial Vols., efficiency, smearing, resolution, quenchings, etc.

Expected signal in underground detectors

$$\frac{dN(t)}{dt} = N_{tar} \int_{E_{th_d}}^{E_{max}} dE \int_{E_{th_r}}^{\infty} dE_\nu \int_0^{\infty} dE' \epsilon(E') \frac{dF_\nu}{dE_\nu}(E_\nu, t) \frac{d\sigma}{dE'}(E_\nu, E') G(E, E', \delta),$$

Detector info Thresholds, Fiducial Vols., efficiency, smearing, resolution, quenchings, etc.

Neutrino Fluxes Oscillation schemes, different flavors for different reactions

Expected signal in underground detectors

$$\frac{dN(t)}{dt} = N_{tar}\int_{E_{th_d}}^{E_{max}} dE \int_{E_{th_r}}^{\infty} dE_\nu \int_0^{\infty} dE' \epsilon(E') \frac{dF_\nu}{dE_\nu}(E_\nu,t) \frac{d\sigma}{dE'}(E_\nu,E') G(E,E',\delta),$$

Detector info Thresholds, Fiducial Vols., efficiency, smearing, resolution, quenchings, etc.

Neutrino Fluxes Oscillation schemes, different flavors for different reactions

Nuclear physics → XS CC and NC cross-sections

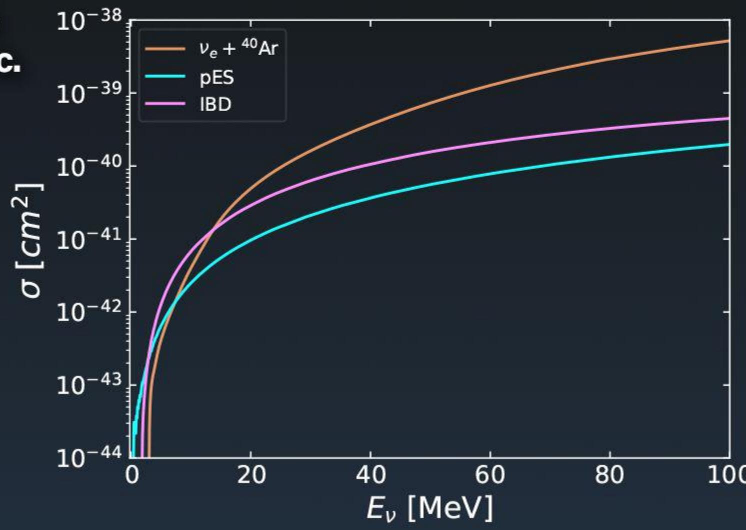

HYPER KAMIOKANDE

Next-generation water Cherenkov detector.
188kt of ultra-pure water.
Dominant channel: $\bar{\nu_e} + p \to n + e^+$

$$E_{th_r} = 1.806\,\mathrm{MeV} \qquad E_{th_d} = 7\,\mathrm{MeV} \;\; E_{max} = 100\,\mathrm{MeV}$$

$$\delta/\mathrm{MeV} = -0.0839 + 0.349\sqrt{E'/\mathrm{MeV}} + 0.0397E'/\mathrm{MeV}$$

DUNE

Four 10-kt liquid argon time projection chambers (LArTPCs) Dominant channel: $\nu_e +^{40}\mathrm{Ar} \to \mathrm{e}^- +^{40}\mathrm{K}^*$

$$E_{th_d} = 5\,\mathrm{MeV} \;\; \mathrm{E_{max}} = 100\,\mathrm{MeV}$$

JUNO

Next-generation liquid scintillator
C6H5CnH2n+1 where n is 95% 9-12, 5% 13-14

$$\bar{\nu_e} + p \to n + e^+$$

$$\nu + p \to \nu' + p$$

$$\frac{d\sigma}{dE'}(E_\nu, E') = \frac{G_F^2 m_p}{2\pi E_\nu^2}\left[(C_V \pm C_A)^2 E_\nu^2 + (C_V \mp C_A)(E_\nu - E')^2 - (C_V^2 - C_A^2) m_p E'\right]$$

$$E_\nu^{min} = \frac{E' + \sqrt{E'(E'+2m_p)}}{2} \qquad \delta = 3\%\sqrt{E'} \qquad E_{th_d} = 0.2\,\mathrm{MeV} \;\; \mathrm{E_{max}} = 60\,\mathrm{MeV}$$

NUMERICAL TOOLS DEVELOPED

BASED ON SNTOOLS AND SNEWPY + OUR CONTRIBUTIONS

Neutrino signal calculations:

&

Statistical analysis:

Neutrino signal as function of E and t
+ new detectors
+ new cross sections
+ smearing
+ detector characteristics
  (efficiency, thresholds, quenchings, fiducial volumes, etc)
+ different oscillation schemes
+ different initial SN models

Montecarlo simulation
+ likelihoods
+ bayes factors
+ model distinguishability analysis

SN Models

2D Boltzmann-radiation-hydrodynamics models (9)
[suyimoshi, yamada, Nagakura]

EoS:
Furusawa and Togashi (FT),
Furusawa and Shen (FS),
Lattimer and Swesty (LS)
11.2, 15, 27 $M_\odot$
With and without rotation

3D Princenton models (9)
[Burrows, Vartanyan]

EoS: SFHo
9,10,12,13,14,15,19,25,60 $M_\odot$
Non rotationals

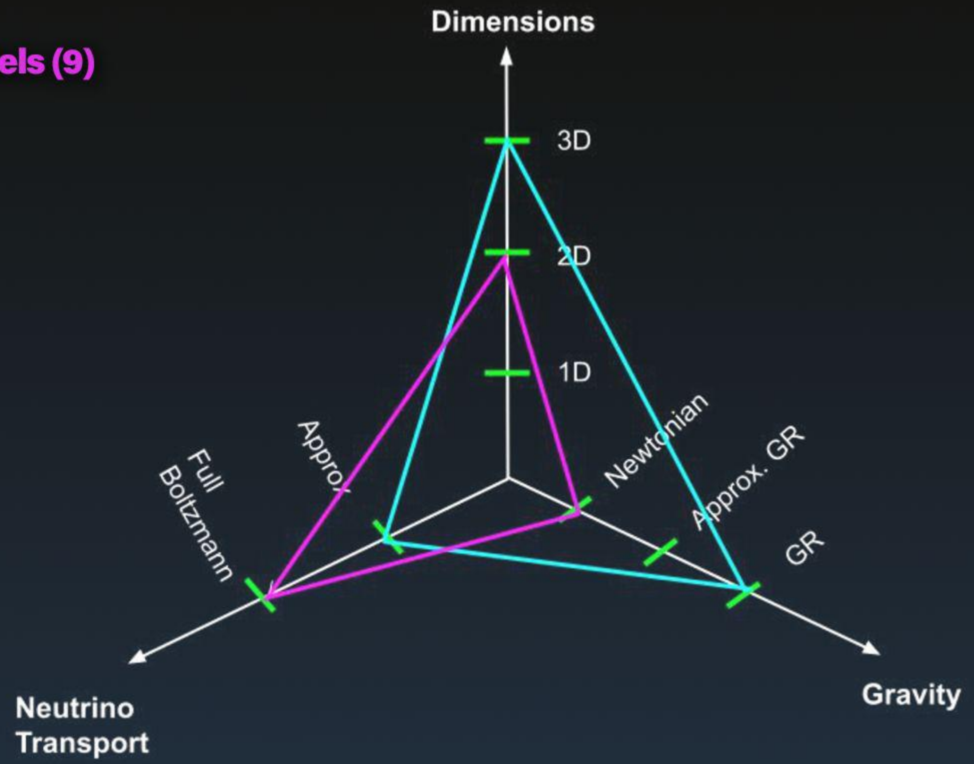

SN Models spectral parameters

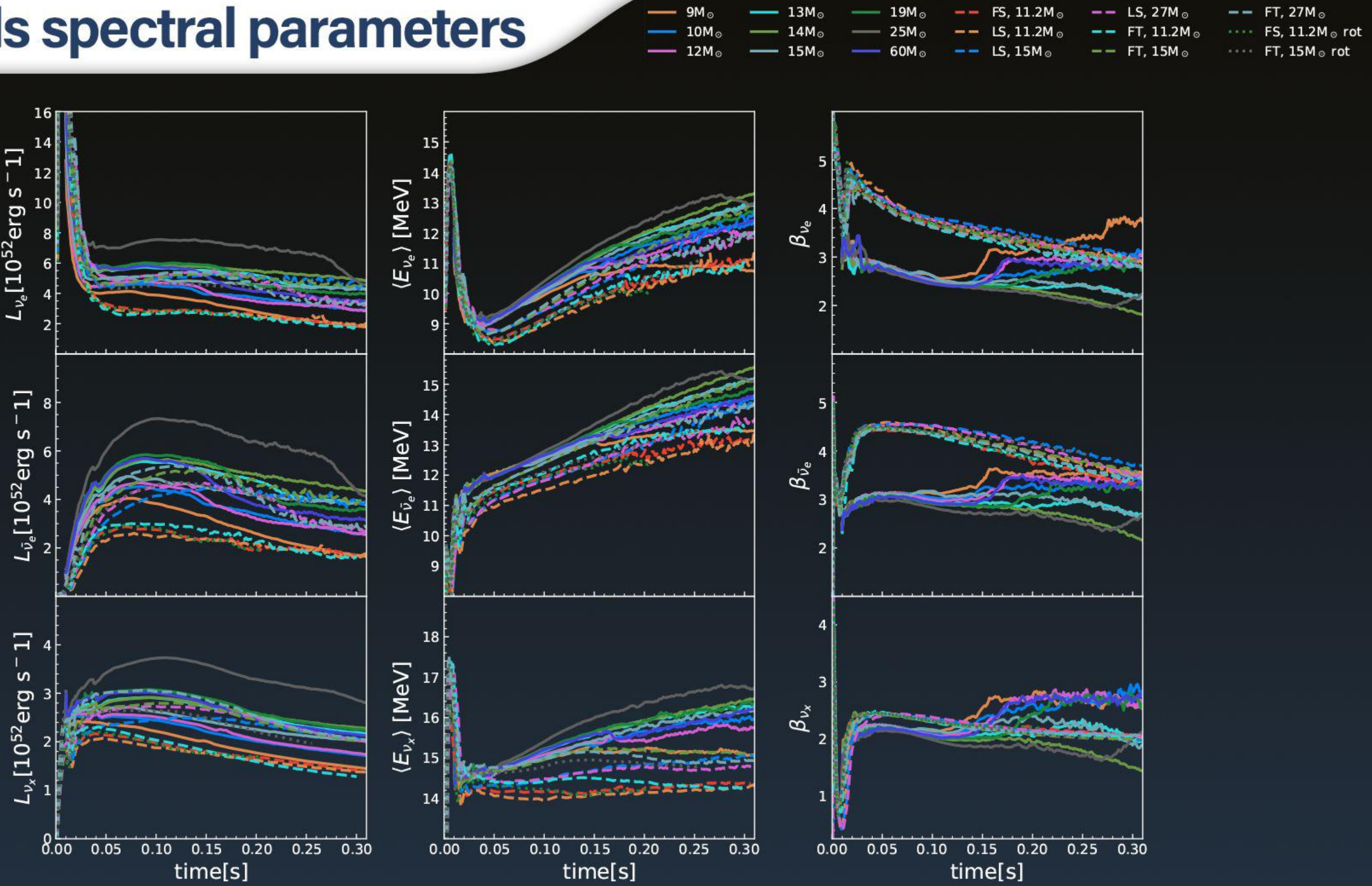

Neutrino signal results

18 SN models:
3D Princeton (Fornax)
2D Boltzmann

Detectors:
HK - IBD channel
DUNE - nue + Ar channel
JUNO - IBD + pES channel

Neutrino mixing:
No oscillation(NO)
NMO
IMO

Event distribution with time or E
Cumulative number of events
Total number of events

(Tfin=300ms and d=10kpc)

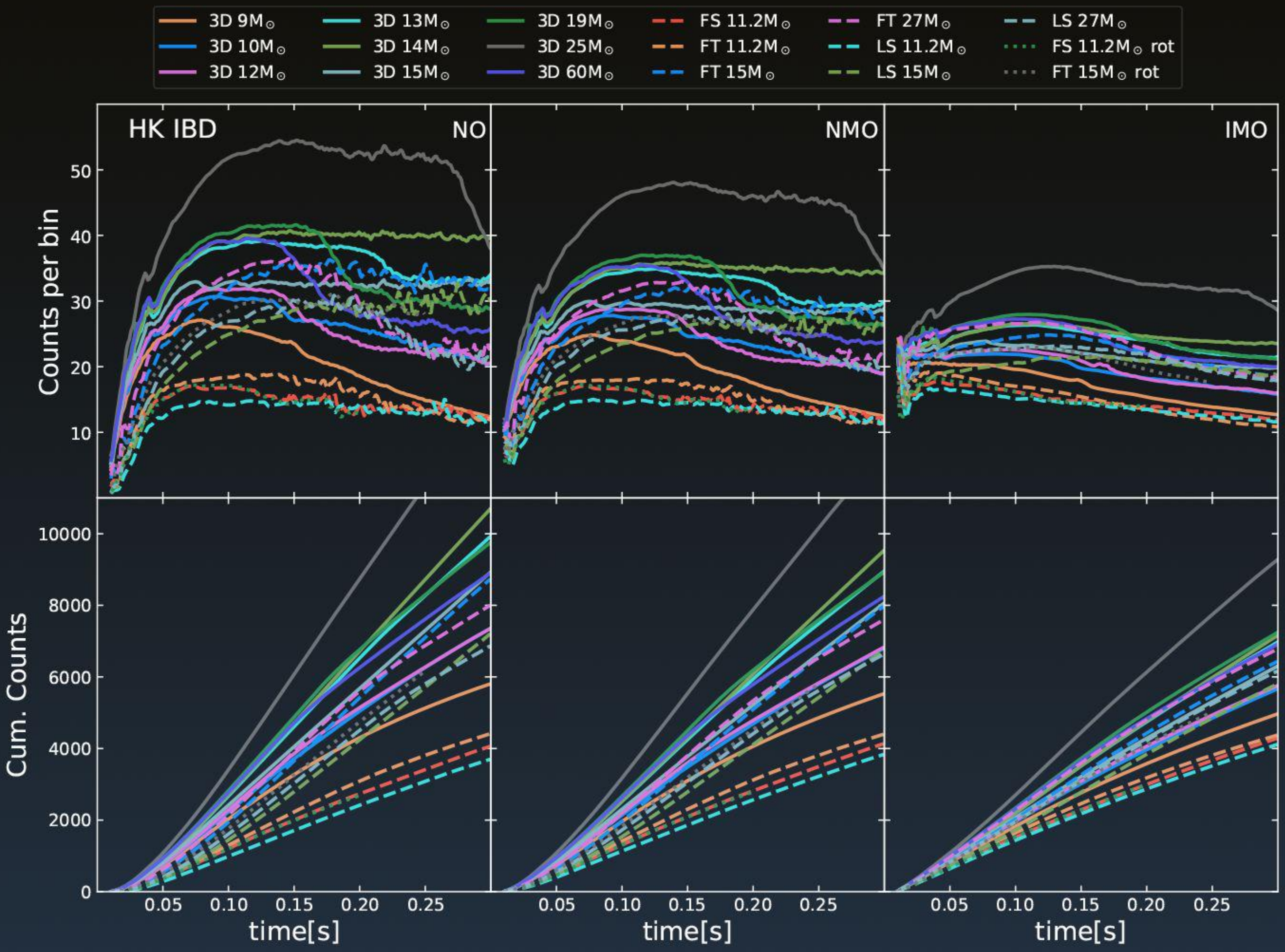

3D 9M$_\odot$
3D 10M$_\odot$
3D 12M$_\odot$
3D 13M$_\odot$
3D 14M$_\odot$
3D 15M$_\odot$
3D 19M$_\odot$
3D 25M$_\odot$
3D 60M$_\odot$
FS 11.2M$_\odot$
FT 11.2M$_\odot$
FT 15M$_\odot$
FT 27M$_\odot$
LS 11.2M$_\odot$
LS 15M$_\odot$
LS 27M$_\odot$
FS 11.2M$_\odot$ rot
FT 15M$_\odot$ rot
HK IBD
NO
NMO
IMO
Counts per bin
Cum. Counts
time[s]

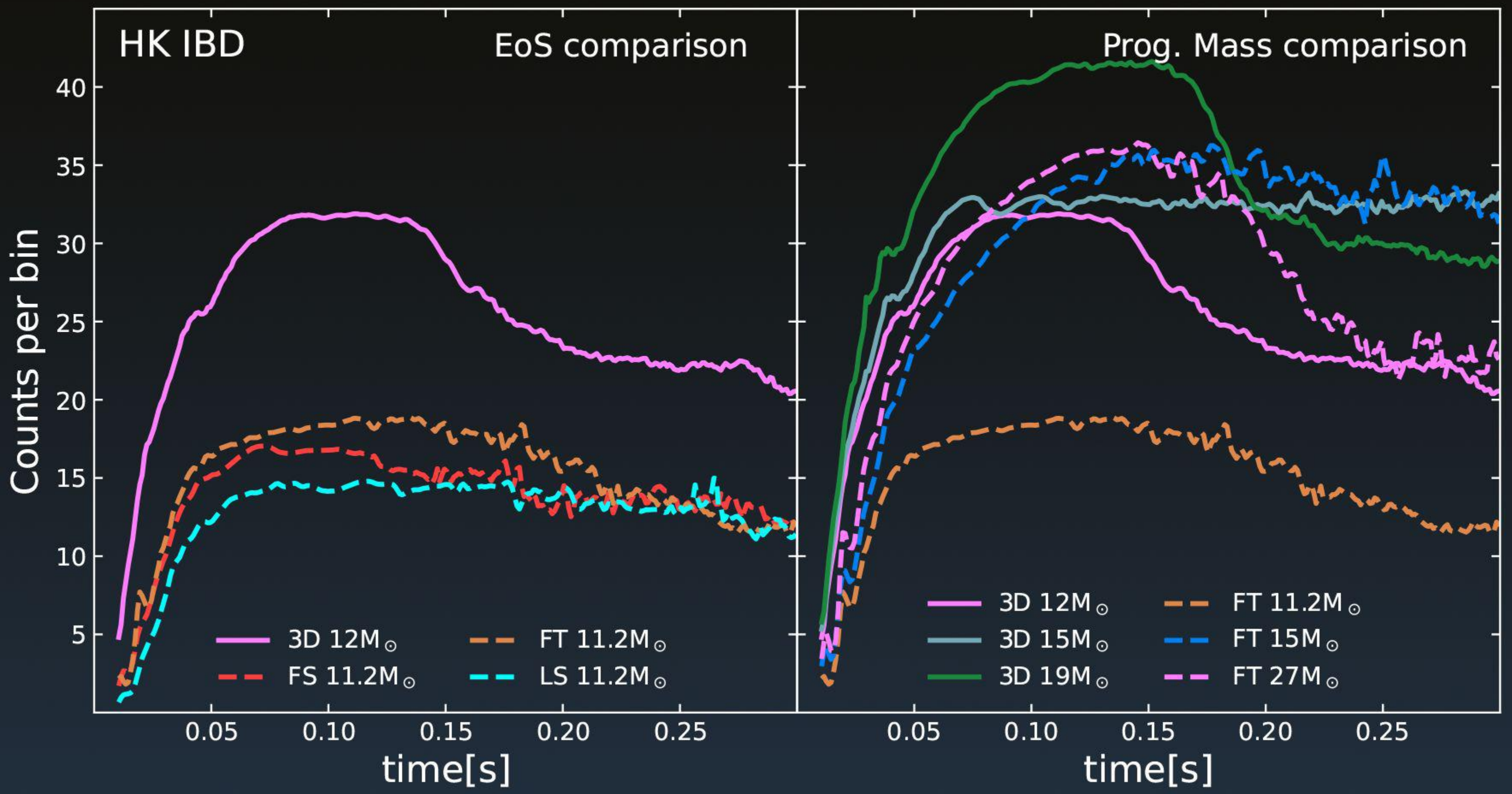

HK IBD
EoS comparison
Prog. Mass comparison
Counts per bin
time[s]
time[s]
3D 12M$_\odot$
FS 11.2M$_\odot$
FT 11.2M$_\odot$
LS 11.2M$_\odot$
3D 12M$_\odot$
3D 15M$_\odot$
3D 19M$_\odot$
FT 11.2M$_\odot$
FT 15M$_\odot$
FT 27M$_\odot$

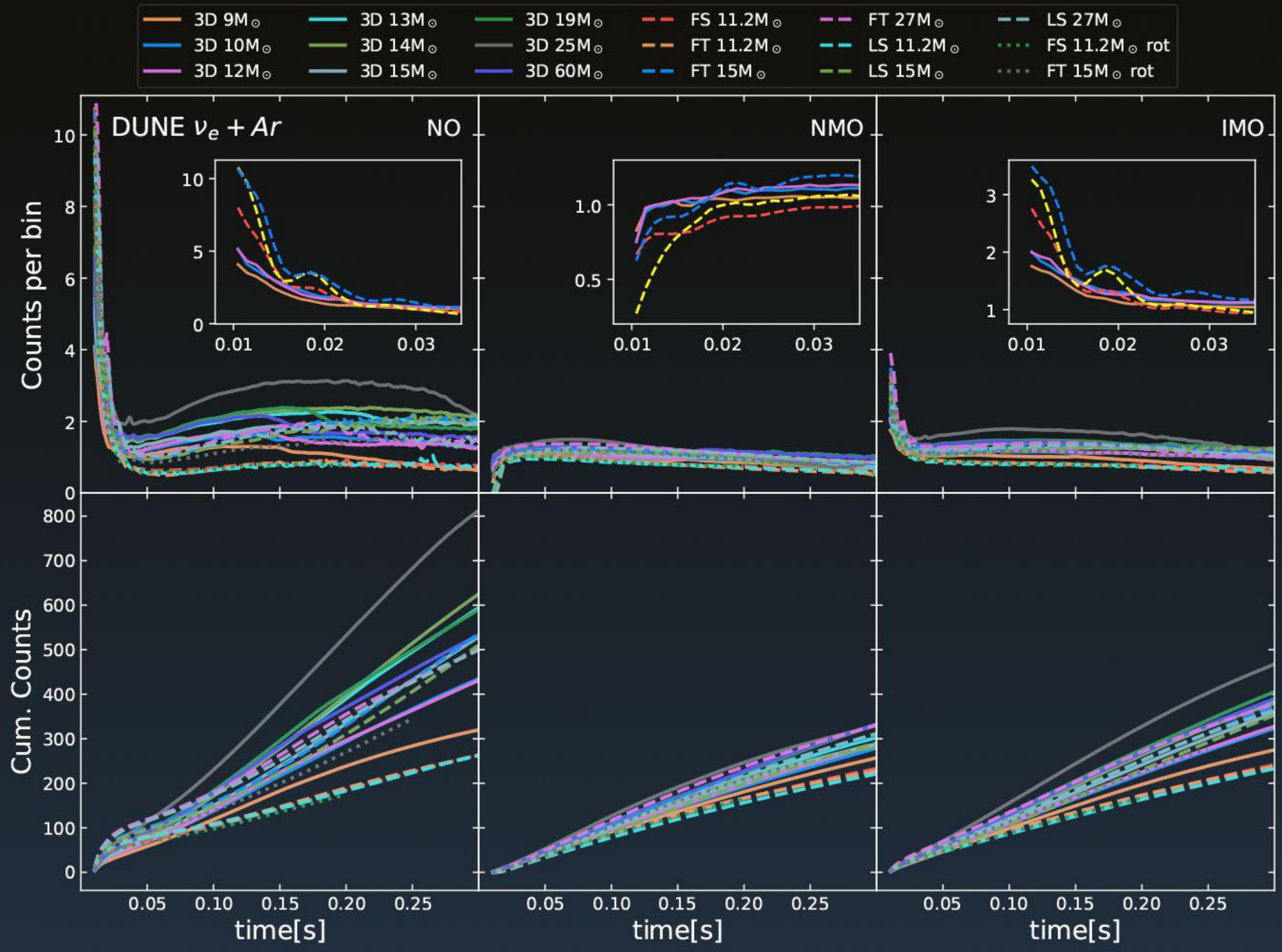
3D 9M$_\odot$
3D 10M$_\odot$
3D 12M$_\odot$
3D 13M$_\odot$
3D 14M$_\odot$
3D 15M$_\odot$
3D 19M$_\odot$
3D 25M$_\odot$
3D 60M$_\odot$
FS 11.2M$_\odot$
FT 11.2M$_\odot$
FT 15M$_\odot$
FT 27M$_\odot$
LS 11.2M$_\odot$
LS 15M$_\odot$
LS 27M$_\odot$
FS 11.2M$_\odot$ rot
FT 15M$_\odot$ rot
DUNE $\nu_e + Ar$
NO
NMO
IMO
Counts per bin
Cum. Counts
time[s]

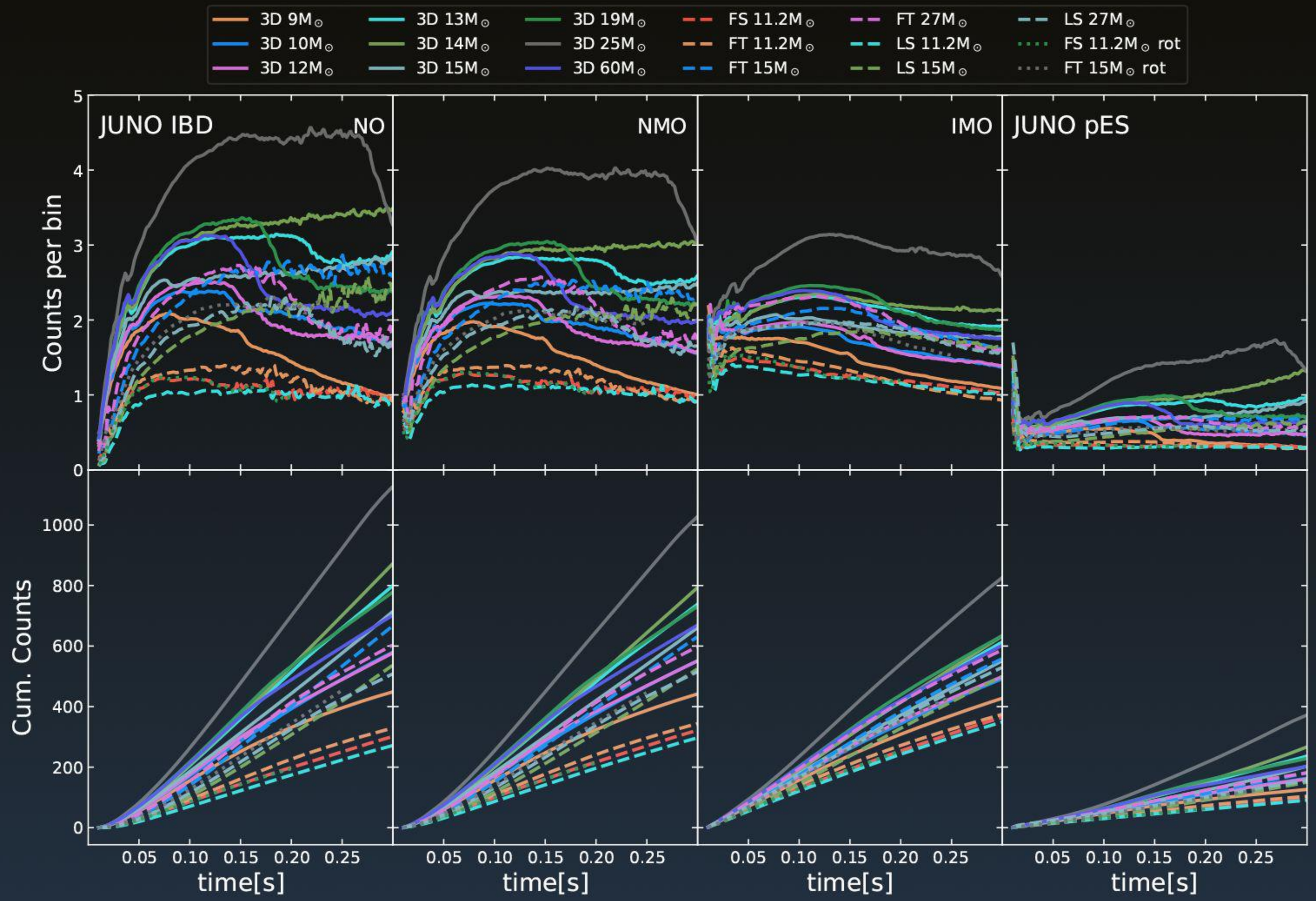

3D 9M☉
3D 10M☉
3D 12M☉
3D 13M☉
3D 14M☉
3D 15M☉
3D 19M☉
3D 25M☉
3D 60M☉
FS 11.2M☉
FT 11.2M☉
FT 15M☉
FT 27M☉
LS 11.2M☉
LS 15M☉
LS 27M☉
FS 11.2M☉ rot
FT 15M☉ rot
JUNO IBD
NO
NMO
IMO
JUNO pES
Counts per bin
Cum. Counts
time[s]

Neutrino signal results useful correlation

TONE: energy- and flavor-integrated time-cumulative neutrino radiation up to a given post-bounce time.

$$F_{\bar{\nu}_e} = \bar{P}_e F^0_{\bar{\nu}_e} + (1 - \bar{P}_e) F^0_{\bar{\nu}_x}$$

Pe ~ 0.7 NMO; 0.3 IMO

Fits with 1st or 2nd order polynomials.

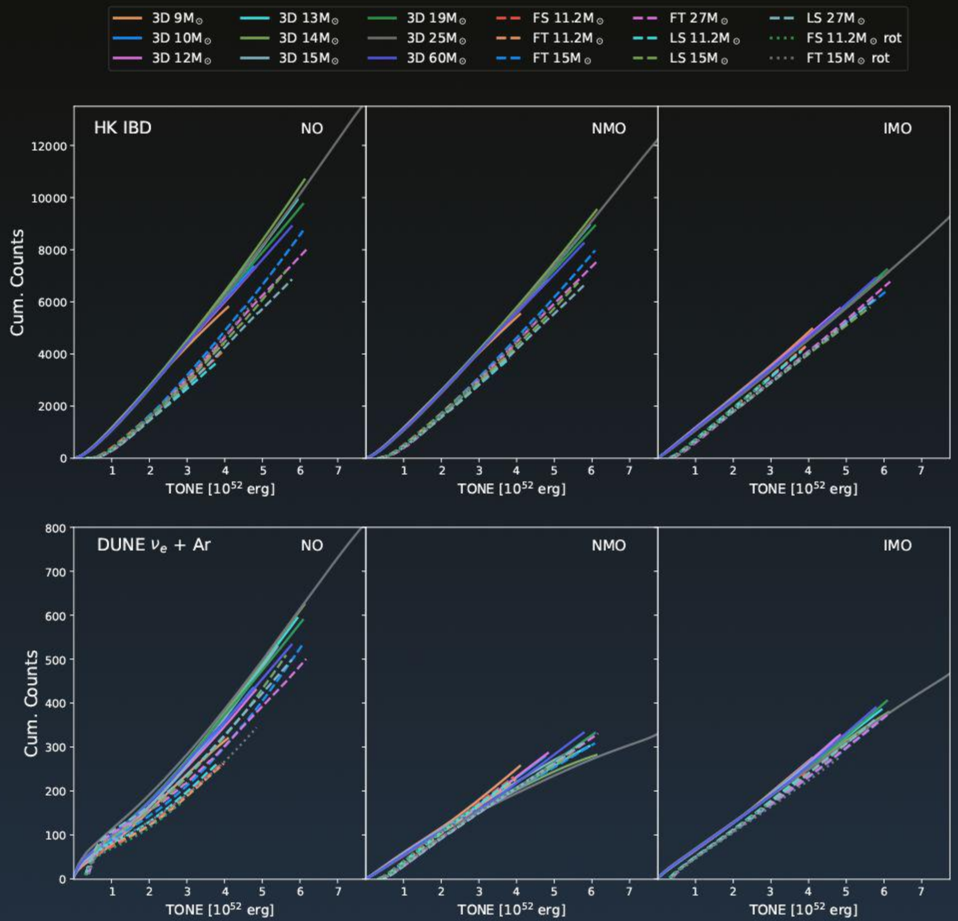

Neutrino signal results useful correlation

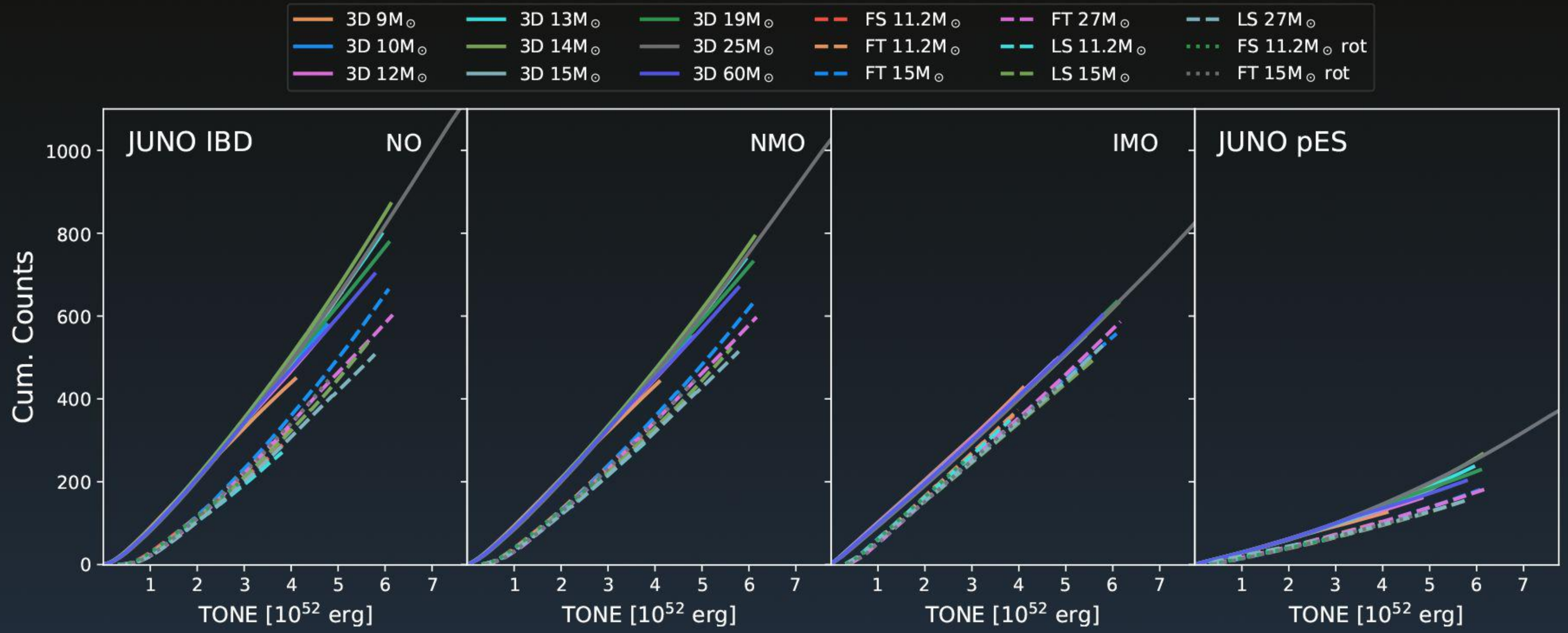

Neutrino signal results useful correlation

Cumulative events → TONE → PNS properties

Correlation between TONE and PNS mass/radius

"Efficient method for estimating the time evolution of the proto-neutron star mass and radius from a supernova neutrino signal" [Nagakura & Vartanyan 2022]

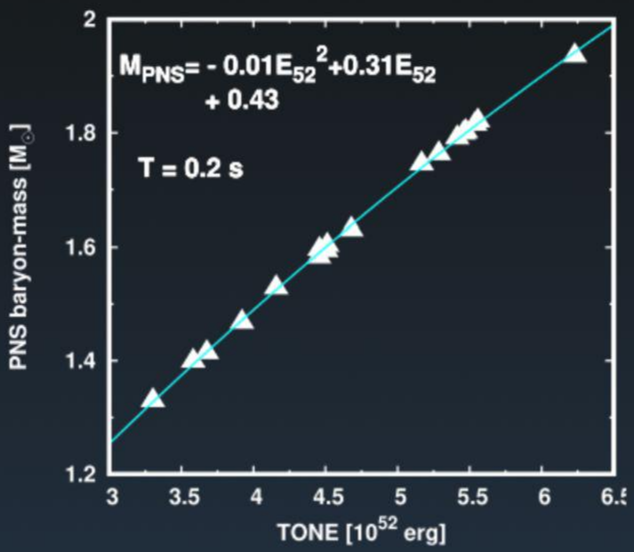

Nagakura & Vartanyan 2022

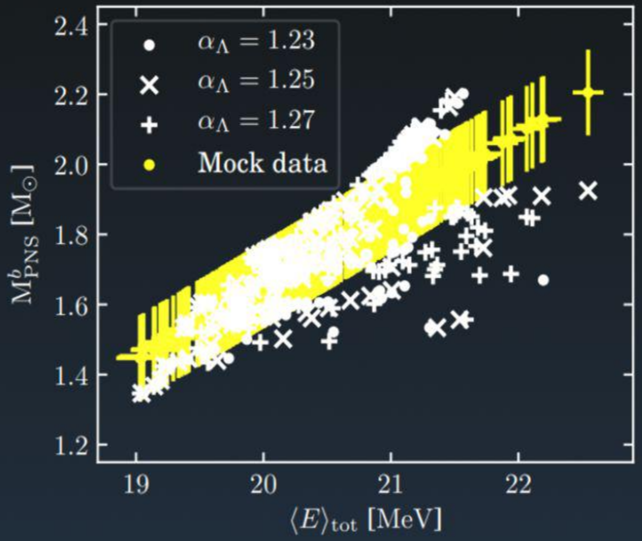

Warren et al. 2020

SN model discrimination

- Following [Olsen & Qian 2021]: Bayes factors as strength of evidence for model distinguishability
- Comparison between models of our dataset
- Detectors HK, DUNE and JUNO (pES channel did not present sensitivity)
- Different mass orderings

We explored discrimination power regarding 3 aspects:

1. EoS
2. Progenitor Mass
3. Neutrino mass ordering

SN model discrimination

Probability distribution for an event to be observed at time t with energy E, for an specific emission model Mj:

$$p(E,t|M_j) = \frac{1}{\langle N \rangle} \frac{d^2N}{dtdE}$$

Extended maximum likelihood [Barlow 1990]:

$$\mathcal{L}(D|M_j) = \frac{e^{-\langle N \rangle} \langle N \rangle^N}{N!} \prod_{i=1}^{N} p(E_i, t_i|M_j)$$

$$\mathcal{B}_{\alpha\beta} = \frac{\mathcal{L}(D|M_\alpha)}{\mathcal{L}(D|M_\beta)}$$

$\ln \mathcal{B}_{\alpha\beta}$	Interpretation
0 to 1	Not worth more than a bare mention
1 to 3	Positive evidence favoring M_α
3 to 5	Strong evidence favoring M_α
> 5	Very Strong evidence favoring M_α

By executing this procedure a total of 10^4 times and leveraging our Monte Carlo simulated signals, we are able to compute both the mean $\langle \ln \mathcal{B}_{\alpha\beta} \rangle$ and the standard deviation $\sigma(\ln \mathcal{B}_{\alpha\beta})$ across all pairs of our model instances. To discern a substantial preference for M_α over M_β, we establish a threshold of $\ln \mathcal{B}_{\alpha\beta} > 5$

Example case: EoS discrimination

IBD channel at HK

Models: 2D, M=11.2 $M_\odot$

1. **True model: FS, other: FT**
2. **True model: FT, other: FS**

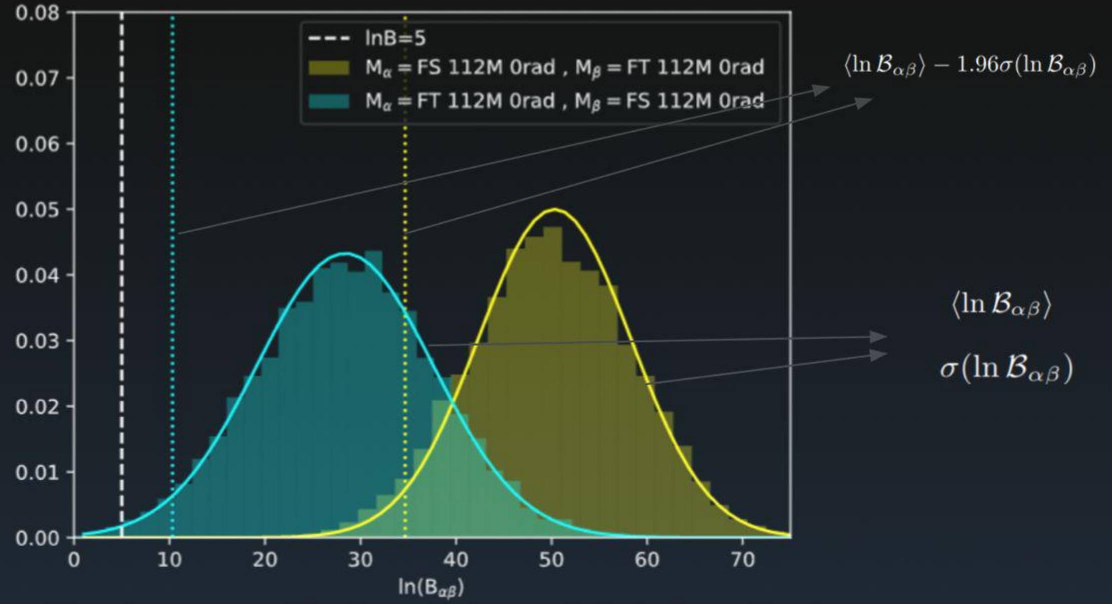

Binned outcomes of the Monte Carlo sample for both model pairs

Models distinguishable at a 95% CL if:

$$\langle \ln \mathcal{B}_{\alpha\beta} \rangle - 1.96\sigma(\ln \mathcal{B}_{\alpha\beta}) > 5$$

EoS discrimination

HK IBD			DUNE ν_e + Ar		JUNO IBD	
M_α/M_β	FT 11.2M$_\odot$	LS 11.2M$_\odot$	FT 11.2M$_\odot$	LS 11.2M$_\odot$	FT 11.2M$_\odot$	LS 11.2M$_\odot$
FS 11.2M$_\odot$						
NO	**39.34 ± 8.62**	**56.65 ± 10.29**	3.49 ± 2.69	1.81 ± 1.89	3.71 ± 5.72	4.52 ± 6.57
NMO	**27.38 ± 6.97**	**27.42 ± 8.14**	0.55 ± 1.18	0.82 ± 0.86	2.05 ± 5.46	2.28 ± 6.06
IMO	**22.17 ± 6.81**	18.45 ± 7.44	0.65 ± 1.49	0.94 ± 0.93	2.02 ± 4.48	1.03 ± 3.38
FT 11.2M$_\odot$						
NO		**141.75 ± 16.08**		2.37 ± 2.20		11.67 ± 7.85
NMO		**76.36 ± 12.53**		0.64 ± 1.57		6.40 ± 6.67
IMO		**29.58 ± 7.78**		0.84 ± 1.59		2.72 ± 5.30
M_α/M_β	LS 15M$_\odot$		LS 15M$_\odot$		LS 15M$_\odot$	
FT 15M$_\odot$						
NO	**278.94 ± 22.49**		2.95 ± 2.63		23.97 ± 10.48	
NMO	**171.71 ± 17.93**		1.01 ± 2.15		15.26 ± 9.64	
IMO	**73.47 ± 12.40**		1.71 ± 2.16		6.42 ± 6.82	
M_α/M_β	LS 27M$_\odot$		LS 27M$_\odot$		LS 27M$_\odot$	
FT 27M$_\odot$						
NO	**216.62 ± 20.14**		2.44 ± 2.25		18.39 ± 9.95	
NMO	**139.11 ± 17.05**		1.24 ± 2.07		11.81 ± 9.28	
IMO	**71.25 ± 12.41**		1.28 ± 2.04		6.26 ± 6.78	

Prog. Mass discrimination

	HK IBD		DUNE ν_e + Ar		JUNO IBD	
M_α / M_β	FT 15$M_\odot$	FT 27$M_\odot$	FT 15$M_\odot$	FT 27$M_\odot$	FT 15$M_\odot$	FT 27$M_\odot$
FT 11.2$M_\odot$						
NO	**1572.51 ± 59.41**	**1071.60 ± 47.85**	**114.30 ± 16.75**	**83.90 ± 13.52**	**126.98 ± 17.94**	**83.41 ± 15.15**
NMO	**1159.26 ± 48.98**	**882.97 ± 42.88**	13.84 ± 6.31	**20.24 ± 7.16**	**94.51 ± 15.84**	**70.99 ± 13.63**
IMO	**467.46 ± 31.33**	**559.28 ± 34.08**	**34.74 ± 8.89**	**34.30 ± 8.75**	**43.18 ± 11.11**	**50.89 ± 11.82**
FT 15$M_\odot$						
NO		**178.36 ± 19.33**		13.79 ± 5.46		15.28 ± 7.85
NMO		**97.01 ± 14.01**		2.89 ± 1.40		8.07 ± 7.50
IMO		**22.03 ± 6.53**		2.06 ± 2.00		4.13 ± 3.08
M_α / M_β	LS 15$M_\odot$	LS 27$M_\odot$	LS 15$M_\odot$	LS 27$M_\odot$	LS 15$M_\odot$	LS 27$M_\odot$
LS 11.2$M_\odot$						
NO	**1227.67 ± 52.72**	**994.21 ± 46.24**	**95.42 ± 14.77**	**87.39 ± 14.56**	**94.90 ± 15.96**	**75.47 ± 14.02**
NMO	**885.34 ± 44.49**	**785.81 ± 40.99**	11.04 ± 5.59	16.73 ± 6.47	**69.47 ± 14.02**	**61.21 ± 13.04**
IMO	**342.00 ± 26.36**	**443.39 ± 29.72**	**28.49 ± 7.95**	**30.66 ± 8.33**	**31.29 ± 10.23**	**39.74 ± 11.10**
LS 15$M_\odot$						
NO		**107.34 ± 14.90**		11.42 ± 4.86		8.63 ± 6.66
NMO		**64.12 ± 11.33**		1.49 ± 1.04		6.18 ± 5.07
IMO		**25.66 ± 7.07**		2.07 ± 1.99		4.04 ± 2.21

Prog. Mass discrimination

HK IBD								
M_α/M_β	3D 10M$_\odot$	3D 12M$_\odot$	3D 13M$_\odot$	3D 14M$_\odot$	3D 15M$_\odot$	3D 19M$_\odot$	3D 25M$_\odot$	3D 60M$_\odot$
3D 9M$_\odot$								
NO	280.43 ± 24.27	246.35 ± 22.38	1390.90 ± 56.04	1943.07 ± 70.00	981.31 ± 47.97	1166.78 ± 50.17	2292.04 ± 60.94	727.75 ± 38.72
NMO	189.91 ± 19.98	175.46 ± 18.94	1024.18 ± 48.34	1419.89 ± 59.28	680.76 ± 39.34	918.07 ± 44.20	2073.38 ± 86.26	590.94 ± 35.12
IMO	67.06 ± 11.76	73.49 ± 12.14	461.30 ± 32.03	618.34 ± 38.68	243.70 ± 23.03	504.23 ± 32.69	1638.47 ± 64.10	357.51 ± 26.66
3D 10M$_\odot$								
NO		17.53 ± 6.01	466.80 ± 30.69	835.34 ± 42.47	241.81 ± 22.74	370.38 ± 27.24	2195.03 ± 70.97	171.15 ± 18.36
NMO		10.99 ± 4.81	361.37 ± 27.84	629.84 ± 37.79	170.00 ± 19.19	315.86 ± 25.51	1812.26 ± 63.69	154.29 ± 17.63
IMO		5.51 ± 3.39	188.28 ± 20.02	309.79 ± 26.73	65.32 ± 11.94	218.43 ± 21.10	1106.25 ± 50.71	133.42 ± 16.06
3D 12M$_\odot$								
NO			528.85 ± 33.10	919.08 ± 45.32	301.92 ± 25.58	386.09 ± 27.89	2290.79 ± 74.03	152.24 ± 17.34
NMO			392.90 ± 28.97	674.41 ± 39.15	203.12 ± 20.89	318.24 ± 25.34	1853.75 ± 64.91	138.18 ± 16.53
IMO			188.44 ± 20.34	315.18 ± 27.34	71.81 ± 12.63	202.61 ± 20.45	1092.95 ± 51.16	113.20 ± 14.88
3D 13M$_\odot$								
NO				78.06 ± 12.74	82.11 ± 12.22	66.56 ± 11.92	702.07 ± 37.46	212.06 ± 21.07
NMO				56.54 ± 10.90	67.34 ± 11.35	42.81 ± 9.44	598.39 ± 34.80	131.52 ± 16.86
IMO				30.55 ± 7.90	46.49 ± 9.64	26.83 ± 7.39	407.86 ± 29.13	52.51 ± 10.58
3D 14M$_\odot$								
NO					215.41 ± 20.13	247.49 ± 23.71	412.43 ± 28.16	492.10 ± 33.21
NMO					171.55 ± 18.57	166.25 ± 19.01	370.80 ± 27.14	323.84 ± 26.92
IMO					102.13 ± 14.51	91.74 ± 14.15	297.41 ± 24.47	141.62 ± 17.93
3D 15M$_\odot$								
NO						148.39 ± 17.29	1155.14 ± 48.64	173.27 ± 18.82
NMO						114.82 ± 14.92	991.88 ± 44.82	107.86 ± 14.82
IMO						94.19 ± 13.65	693.22 ± 38.39	64.98 ± 11.23
3D 19M$_\odot$								
NO							923.26 ± 45.41	85.46 ± 13.09
NMO							693.22 ± 38.39	57.81 ± 10.85
IMO							414.05 ± 30.46	24.89 ± 7.15
3D 25M$_\odot$								
NO								1437.57 ± 58.10
NMO								1103.76 ± 49.57
IMO								581.59 ± 36.80

Mass ordering discrimination

	HK IBD	DUNE ν_e + Ar	JUNO IBD
M_α/M_β	IMO	IMO	IMO
FS 11.2M$_\odot$			
NMO	421.25 ± 24.84	13.17 ± 4.78	36.64 ± 9.85
FT 11.2M$_\odot$			
NMO	484.19 ± 29.37	17.17 ± 5.14	41.80 ± 10.30
FT 15M$_\odot$			
NMO	1156.26 ± 48.89	30.76 ± 6.50	74.37 ± 15.90
FT 27M$_\odot$			
NMO	953.31 ± 42.51	30.05 ± 6.44	68.66 ± 14.65
LS 11.2M$_\odot$			
NMO	473.83 ± 27.32	18.18 ± 5.24	41.61 ± 10.49
LS 15M$_\odot$			
NMO	1021.29 ±44.53	34.29 ± 6.67	72.24 ± 14.32
LS 27M$_\odot$			
NMO	914.57 ± 40.71	35.79 ± 6.82	69.24 ± 14.33
3D 9M$_\odot$			
NMO	477.65 ± 30.86	9.57 ± 3.85	30.11 ± 10.42
3D 10M$_\odot$			
NMO	626.42 ± 37.26	14.59 ± 4.31	39.04 ± 11.89
3D 12M$_\odot$			
NMO	626.27 ± 35.97	14.39 ± 4.35	37.32 ± 12.22
3D 13M$_\odot$			
NMO	946.44 ± 45.47	25.37 ± 5.15	56.49 ± 14.59
3D 14M$_\odot$			
NMO	1099.72 ± 50.60	30.97 ± 5.39	64.07 ± 15.45
3D 15M$_\odot$			
NMO	849.89 ± 43.69	20.82 ± 4.86	50.80 ± 13.97
3D 19M$_\odot$			
NMO	868.20 ± 42.97	20.27 ± 3.58	52.55 ± 13.73
3D 25M$_\odot$			
NMO	1384.53 ± 55.17	47.57 ± 6.33	80.95 ± 17.60
3D 60M$_\odot$			
NMO	766.91 ± 39.89	19.09 ± 4.79	45.63 ± 13.26

Neutronization burst only

DUNE ν_e + Ar	
M_α/M_β	IMO
FS 11.2M$_\odot$	
NMO	8.49 ± 2.97
FT 11.2M$_\odot$	
NMO	12.55 ± 3.08
FT 15M$_\odot$	
NMO	13.80 ± 3.45
FT 27M$_\odot$	
NMO	17.80 ± 3.60
LS 11.2M$_\odot$	
NMO	13.06 ± 2.77
LS 15M$_\odot$	
NMO	17.08 ± 2.86
LS 27M$_\odot$	
NMO	21.70 ± 2.98
3D 9M$_\odot$	
NMO	6.64 ± 2.32
3D 10M$_\odot$	
NMO	8.14 ± 2.42
3D 12M$_\odot$	
NMO	8.20 ± 2.45
3D 13M$_\odot$	
NMO	10.58 ± 2.64
3D 14M$_\odot$	
NMO	9.88 ± 2.67
3D 15M$_\odot$	
NMO	9.13 ± 2.56
3D 19M$_\odot$	
NMO	11.68 ± 2.76
3D 25M$_\odot$	
NMO	15.24 ± 3.07
3D 60M$_\odot$	
NMO	11.40 ± 2.74

Conclusions:

- Nu-signal from Boltzmann-radiation-hydrodynamics models studied for the very first time
- Systematic exploration across 3 detectors and comparison with Fornax 3D simulations
- Correlation between the TONE and the cumulative count statistics:
  primarily influenced by the massive lepton neutrinos that originate from the source.
- **The strength of this correlation** is **shaped by the surviving probabilities,**
  which highlights the crucial aspect of accounting for neutrino oscillations in the analysis
- The correlation between all models is notably **narrower at DUNE**
- The forthcoming Galactic SN's neutrino signal will provide us with the means
  to differentiate among a diverse array of models
- **HK: optimal detector for distinguishing between models** (mass ordering, EoS and Mprog)

Future work:

- Include more SN initial models in the study
- Further explore the correlation. Incorporate errors, Ymu?, supplement the study with hydrodynamic information, etc
- Improve the neutrino oscillation treatment (collective effects?, sterile neutrinos?, non-adiabatica transformations? etc)
- Explore other neutral channels
- DUNE cross sections → most of the predictions (99% in literature) are made using SNOwgloBEs Xs [E. Kolbe et al. 2003] → several new argon XS calculations. Effects on expected DUNE signal?
- Hybrid EoS, hadron-quark phase transition: signatures in the neutrino and GW signals?
- New observable definitions:

  Ratios of events in different detection channels (CC/NC). [Saez et al. 2310.19939]

Backup slides

-)Furusawa and Shen (FS): based on the Shen EoS [Shen:1998]. Nuclear statistical equilibrium (NSE) is considered for the ensemble of nuclei in order to calculate the thermodynamical and statistical properties of nonuniform matter.
The Shen EoS, models the strong interaction by the RMF theory with the TM1 parameter set.

-)Lattimer and Swesty (LS): based on the liquid drop model of the nuclei and the Skyrme-type interaction. As for the composition, Lattimer and Swesty [Lattimer:1991] assume that the heavy nuclei are represented by a single nuclear species (single nuclear approximation, SNA), and only the alpha particle is considered as the light nuclei.

-)Furusawa and Togashi (FT): based on Togashi variational method but NSE is assumed [Togashi:2017].

-)SFHo: based on the relativistic mean field (RMF) theory whose parameters are tuned to fit the observations[Steiner:2013]. (do not employ the SNA in the vicinity of the saturation density. Rather, several thousand nuclei are taken into account, whose masses and binding energies, when available, are taken from experiment.)

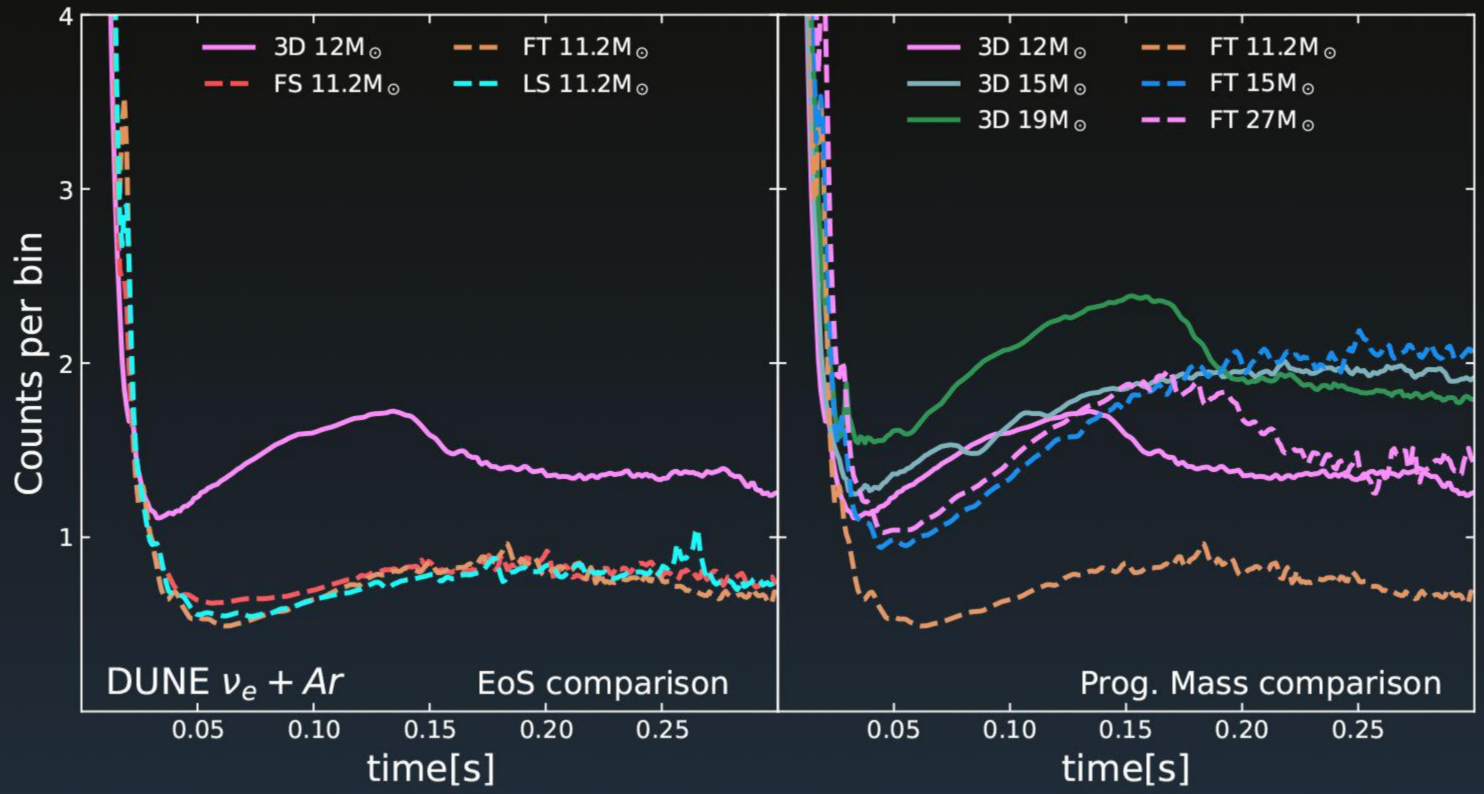

Counts per bin
3D 12M⊙
FS 11.2M⊙
FT 11.2M⊙
LS 11.2M⊙
DUNE $\nu_e + Ar$
EoS comparison
time[s]
3D 12M⊙
3D 15M⊙
3D 19M⊙
FT 11.2M⊙
FT 15M⊙
FT 27M⊙
Prog. Mass comparison
time[s]

Cherenkov detectors: Charged particles are detected via their Cherenkov light emission. IBD is overwhelmingly dominant in the supernova neutrino energy regime: water Cherenkov detectors are primarily sensitive to the ¯ve component of the flux. The primary observable is the Cherenkov radiation of the IBD positron.

Scintillator detectors are composed of hydrocarbons, which have the approximate chemical formula CnH2n. The energy loss of charged particles is observed via light emitted from deexcitation of molecular energy levels, and a very large number of photons may be released.

LARTPC: Liquid argon has a particular sensitivity to the ve component of a supernova neutrino burst, via the dominant interaction, CC absorption of ve on 40Ar, for which the observable is the e − plus deexcitation products from the excited 40K∗ final state.

$$\ln B_{\alpha\beta} = N \ln \frac{\langle N \rangle_\alpha}{\langle N \rangle_\beta} - \Delta_{\alpha\beta} + \sum_{i=1}^{N} \ln \frac{p(E_i, t_i | M_\alpha)}{p(E_i, t_i | M_\beta)},$$

$$\frac{\langle \ln B_{\alpha\beta} \rangle}{\langle N \rangle_\alpha} = \ln \frac{\langle N \rangle_\alpha}{\langle N \rangle_\beta} - \frac{\Delta_{\alpha\beta}}{\langle N \rangle_\alpha} + \left\langle \ln \frac{p(E, t | M_\alpha)}{p(E, t | M_\beta)} \right\rangle_\alpha$$

$$\frac{\sigma[\ln B_{\alpha\beta}]}{\sqrt{\langle N \rangle_\alpha}} = \left[\left(\ln \frac{\langle N \rangle_\alpha}{\langle N \rangle_\beta} \right)^2 + 2 \ln \frac{\langle N \rangle_\alpha}{\langle N \rangle_\beta} \left\langle \ln \frac{p(E, t | M_\alpha)}{p(E, t | M_\beta)} \right\rangle_\alpha + \left\langle \left(\ln \frac{p(E, t | M_\alpha)}{p(E, t | M_\beta)} \right)^2 \right\rangle_\alpha \right]^{1/2},$$

$$\left\langle \ln \frac{p(E, t | M_\alpha)}{p(E, t | M_\beta)} \right\rangle_\alpha = \int_0^{9\text{ s}} dt \int_{E_{\min}}^{\infty} dE\, p(E, t | M_\alpha) \times \ln \frac{p(E, t | M_\alpha)}{p(E, t | M_\beta)}.$$

[Olsen & Qian 2022]

DUNE ν_e + Ar								
M_α/M_β	3D 10M$_\odot$	3D 12M$_\odot$	3D 13M$_\odot$	3D 14M$_\odot$	3D 15M$_\odot$	3D 19M$_\odot$	3D 25M$_\odot$	3D 60M$_\odot$
3D 9M$_\odot$								
NO	**28.67 ± 8.27**	**23.96 ± 7.36**	**104.20 ± 16.98**	**126.69 ± 19.80**	**75.79 ± 14.60**	**94.33 ± 15.26**	**243.06 ± 27.15**	**62.02 ± 11.84**
NMO	2.27 ± 1.01	2.48 ± 1.85	5.20 ± 4.02	5.22 ±0.12	3.71 ± 2.05	4.46 ± 2.20	9.63 ± 4.17	10.41 ± 5.53
IMO	5.15 ± 3.57	5.52 ± 3.54	**20.68 ± 7.91**	18.45 ± 8.49	12.75 ± 6.26	**27.01 ± 8.41**	**50.71 ± 13.81**	**20.98 ± 7.09**
3D 10M$_\odot$								
NO		1.54 ± 1.99	**27.75 ± 8.21**	**40.97 ± 10.53**	13.47 ± 5.91	**25.30 ± 7.45**	**122.87 ± 17.79**	12.18 ± 4.94
NMO		0.60 ± 0.25	3.13 ± 1.42	3.23 ± 0.55	1.65 ± 0.46	5.02 ± 4.07	7.20 ± 5.45	4.92 ± 3.43
IMO		0.78 ± 0.29	5.63 ± 4.40	4.19 ± 5.01	2.75 ± 1.13	9.53 ± 4.93	24.92 ± 10.21	6.37 ± 3.72
3D 12M$_\odot$								
NO			**33.35 ± 9.17**	**47.51 ± 11.54**	18.27 ± 6.95	**28.07 ± 7.95**	**131.66 ± 18.74**	11.82 ± 4.97
NMO			2.92 ± 0.74	3.03 ± 0.96	1.51 ± 0.25	3.78 ± 3.82	6.96 ± 4.01	3.64 ± 3.14
IMO			4.99 ± 4.41	5.04 ± 3.56	2.82 ± 1.38	8.60 ± 4.84	23.30 ± 10.16	5.54 ± 3.55
3D 13M$_\odot$								
NO				2.87 ± 2.55	5.45 ± 3.41	3.18 ± 2.92	**36.61 ± 9.52**	10.81 ± 5.58
NMO				0.73 ± 0.67	1.62 ± 0.49	1.84 ± 1.21	4.17± 1.51	1.29 ± 1.12
IMO				1.09 ± 0.39	2.03 ± 1.20	0.66 ± 0.8	7.15 ± 5.82	1.81 ± 0.29
3D 14M$_\odot$								
NO					9.31 ± 4.89	7.94 ± 5.22	**26.73 ± 7.84**	20.37 ± 7.98
NMO					1.75 ± 0.64	3.26 ± 2.59	4.06 ± 3.67	7.81 ± 1.44
IMO					2.57 ± 0.87	1.38 ± 1.66	8.66 ± 5.23	2.52 ± 0.48
3D 15M$_\odot$								
NO						10.07 ± 4.58	**64.36 ± 12.45**	10.64 ± 5.12
NMO						3.26 ± 2.59	5.67 ± 3.06	3.45 ± 2.09
IMO						3.44 ± 2.77	14.61 ± 7.75	2.15 ± 2.14
3D 19M$_\odot$								
NO							**55.53 ± 10.79**	4.13 ± 3.51
NMO							3.43 ± 0.62	0.99 ± 0.13
IMO							5.53 ± 4.42	1.57 ± 0.45
3D 25M$_\odot$								
NO								**63.21 ± 14.13**
NMO								4.15 ± 1.29
IMO								7.06 ± 3.85

JUNO IBD

M_α/M_β	3D 10$M_\odot$	3D 12$M_\odot$	3D 13$M_\odot$	3D 14$M_\odot$	3D 15$M_\odot$	3D 19$M_\odot$	3D 25$M_\odot$	3D 60$M_\odot$
3D 9$M_\odot$								
NO	**25.87 ± 9.30**	**21.88 ± 8.61**	**128.39 ± 17.89**	**183.91 ± 22.00**	**91.73 ± 15.19**	**103.62 ± 16.09**	**345.09 ± 30.17**	**62.77 ± 13.02**
NMO	17.68 ± 7.70	15.80 ± 7.70	**95.31 ± 14.79**	**135.12 ± 17.98**	**63.88 ± 12.65**	**82.75 ± 14.10**	**275.37 ± 26.02**	**51.72 ± 11.46**
IMO	6.87 ± 4.21	7.40 ± 4.98	**37.61 ± 7.03**	**61.74 ± 12.71**	**24.14 ± 8.44**	**48.14 ± 11.24**	**158.38 ± 19.57**	**33.23 ± 9.99**
3D 10$M_\odot$								
NO		5.51 ± 2.96	**42.21 ± 11.19**	**79.36 ± 14.36**	22.15 ± 8.88	**31.87 ± 9.99**	**202.43 ± 22.22**	13.75 ± 7.78
NMO		4.93 ± 2.13	**33.43 ± 9.76**	**60.19 ± 12.48**	16.11 ± 7.61	**27.73 ± 9.20**	**166.88 ± 19.95**	12.84 ± 6.85
IMO		3.71 ± 1.28	18.40 ± 7.81	**30.60 ± 9.16**	5.75 ± 3.89	20.29 ± 8.24	**105.48 ± 15.91**	11.99 ± 6.86
3D 12$M_\odot$								
NO			**49.57 ± 11.66**	**89.60 ± 15.17**	**28.48 ± 9.86**	**33.92 ± 10.60**	**214.60 ± 22.74**	**12.35 ± 6.98**
NMO			**37.27 ± 10.02**	**65.76 ± 13.07**	**19.54 ± 8.29**	**28.58 ± 9.70**	**173.62 ± 20.31**	11.70 ± 6.41
IMO			18.71 ± 7.81	**31.87 ± 9.46**	6.09 ± 4.07	18.91 ± 8.10	**105.75 ± 16.01**	10.14 ± 6.43
3D 13$M_\odot$								
NO				7.23 ± 4.36	6.93 ± 4.98	7.14 ± 4.77	64.52 ± 13.71	19.72 ± 7.78
NMO				7.18 ± 4.19	6.60 ± 3.94	6.09 ± 3.96	**54.51 ± 13.21**	9.81 ± 5.35
IMO				5.06 ± 3.48	5.71 ± 3.57	4.77 ± 3.15	**38.22 ± 10.38**	6.22 ± 3.64
3D 14$M_\odot$								
NO					16.23 ± 7.98	**25.13 ± 9.18**	**36.47 ± 11.62**	**50.74 ± 11.67**
NMO					13.45 ± 6.55	15.52 ± 6.44	**32.45 ± 10.92**	**33.01 ± 9.72**
IMO					7.06 ± 4.36	5.89 ± 3.89	**27.45 ± 9.53**	8.09 ± 4.07
3D 15$M_\odot$								
NO						12.66 ± 8.42	**105.66 ± 16.99**	16.02 ± 8.69
NMO						10.02 ± 7.18	**91.65 ± 15.69**	8.00 ± 5.59
IMO						8.15 ± 6.62	**65.65 ± 12.99**	6.02 ± 4.64
3D 19$M_\odot$								
NO							**89.22 ± 15.24**	7.29 ± 4.58
NMO							**69.29 ± 13.76**	6.87 ± 4.58
IMO							**39.85 ± 10.17**	4.81 ± 3.36
3D 25$M_\odot$								
NO								**139.92 ± 18.44**
NMO								**106.78 ± 16.44**
IMO								**57.52 ± 11.80**

SN model	$\langle N\rangle_{\mathrm{HK-IBD}}$	$\langle N\rangle_{\mathrm{DUNE}-\nu_e+\mathrm{Ar}}$	$\langle N\rangle_{\mathrm{JUNO-IBD}}$	$\langle N\rangle_{\mathrm{JUNO-pES}}$
FS 11.2$M_\odot$				
NO	4060.73	263.57	300.86	94.52
NMO	4135.24	232.35	321.68	
IMO	4287.04	241.24	364.11	
FT 11.2$M_\odot$				
NO	4412.90	262.40	328.97	103.67
NMO	4399.86	227.22	343.80	
IMO	4373.35	237.25	374.0	
FT 15$M_\odot$				
NO	8729.38	534.59	665.66	180.81
NMO	7972.33	308.52	630.12	
IMO	6430.36	372.89	557.75	
FT 27$M_\odot$				
NO	8001.56	500.24	603.00	181.38
NMO	7597.67	330.55	597.60	
IMO	6775.03	378.87	586.65	
LS 11.2$M_\odot$				
NO	3698.63	262.58	271.05	90.56
NMO	3834.93	220.77	296.67	
IMO	4112.51	232.63	348.84	
LS 15$M_\odot$				
NO	7205.00	509.16	535.97	150.0
NMO	6743.71	290.45	523.79	
IMO	5804.10	352.57	498.98	
LS 27$M_\odot$				
NO	6865.32	499.00	507.86	155.38
NMO	6633.72	311.00	514.81	
IMO	6162.03	364.19	528.99	
FS 11.2$M_\odot$ rot				
NO	2682.33	174.32	194.45	62.65
NMO	2783.44	164.33	213.83	
IMO	2989.51	167.17	253.31	
FT 15$M_\odot$ rot				
NO	6156.31	344.28	452.64	124.11
NMO	5780.72	251.82	445.79	
IMO	5015.67	278.14	431.83	
3D 9$M_\odot$				
NO	5803.79	319.65	448.43	126.17
NMO	5526.81	256.74	441.38	
IMO	5013	263.57	300.86	
3D 10$M_\odot$				
NO	7349.60	434.14	579.05	162.63
NMO	6793.82	278.54	550.26	
IMO	5661.89	322.84	328.97	
3D 12$M_\odot$				
NO	7351.13	430.19	576.43	160.64
NMO	6824.39	286.21	550.70	
IMO	5751.68	534.59	665.66	
3D 13$M_\odot$				
NO	9916.66	593.40	798.33	236.19
NMO	8944.62	302.16	737.07	
IMO	6965.02	385.08	612.31	
3D 14$M_\odot$				
NO	10690.80	624.14	870.83	266.51
NMO	9525.98	281.87	792.17	
IMO	7153.43	379.32	632.21	
3D 15$M_\odot$				
NO	8917.34	528.16	713.04	202.60
NMO	8054.11	288.13	659.56	
IMO	6296.01	356.47	550.63	
3D 19$M_\odot$				
NO	9747.49	589.19	777.31	228.42
NMO	8920.65	331.84	730.03	
IMO	7236.70	405.11	633.74	
3D 25$M_\odot$				
NO	13692.27	811.58	1125.61	371.30
NMO	12235.23	329.90	1026.43	
IMO	9267.60	467.04	825.06	
3D 60$M_\odot$				
NO	8896.73	532.58	701.21	202.49
NMO	8242.20	232.35	668.41	
IMO	6909.17	389.45	601.60	

Correlation fittings:

$$\mathrm{Cum}_{(\mathrm{DUNE-NMO})} = (0.43E^2 + 51.19E)\left(\frac{d}{10kpc}\right)^{-2}\left(\frac{V}{40kt}\right)$$

$$\mathrm{Cum}_{(\mathrm{DUNE-IMO})} = (59.63E + 9.91)\left(\frac{d}{10kpc}\right)^{-2}\left(\frac{V}{40kt}\right)$$

$$\mathrm{Cum}_{(\mathrm{JUNO-IBD-NMO})_{3\mathrm{D}}} = (5.38E^2 + 92.6E)\left(\frac{d}{10kpc}\right)^{-2}\left(\frac{V}{18.25kt}\right)$$

$$\mathrm{Cum}_{(\mathrm{JUNO-IBD-IMO})_{3\mathrm{D}}} = (106.8E - 19.37)\left(\frac{d}{10kpc}\right)^{-2}\left(\frac{V}{18.25kt}\right)$$

$$\mathrm{Cum}_{(\mathrm{JUNO-IBD-NMO})_{2\mathrm{D}}} = (8.05E^2 + 50.75E)\left(\frac{d}{10kpc}\right)^{-2}\left(\frac{V}{18.25kt}\right)$$

$$\mathrm{Cum}_{(\mathrm{JUNO-IBD-IMO})_{2\mathrm{D}}} = (99.26E - 45.5)\left(\frac{d}{10kpc}\right)^{-2}\left(\frac{V}{18.25kt}\right)$$

$$\mathrm{Cum}_{(\mathrm{JUNO-pES})_{3\mathrm{D}}} = (2.31E^2 + 26.12E)\left(\frac{d}{10kpc}\right)^{-2}\left(\frac{V}{18.25kt}\right)$$

$$\mathrm{Cum}_{(\mathrm{JUNO-pES})_{2\mathrm{D}}} = (1.93E^2 + 17.83E)\left(\frac{d}{10kpc}\right)^{-2}\left(\frac{V}{18.25kt}\right)$$

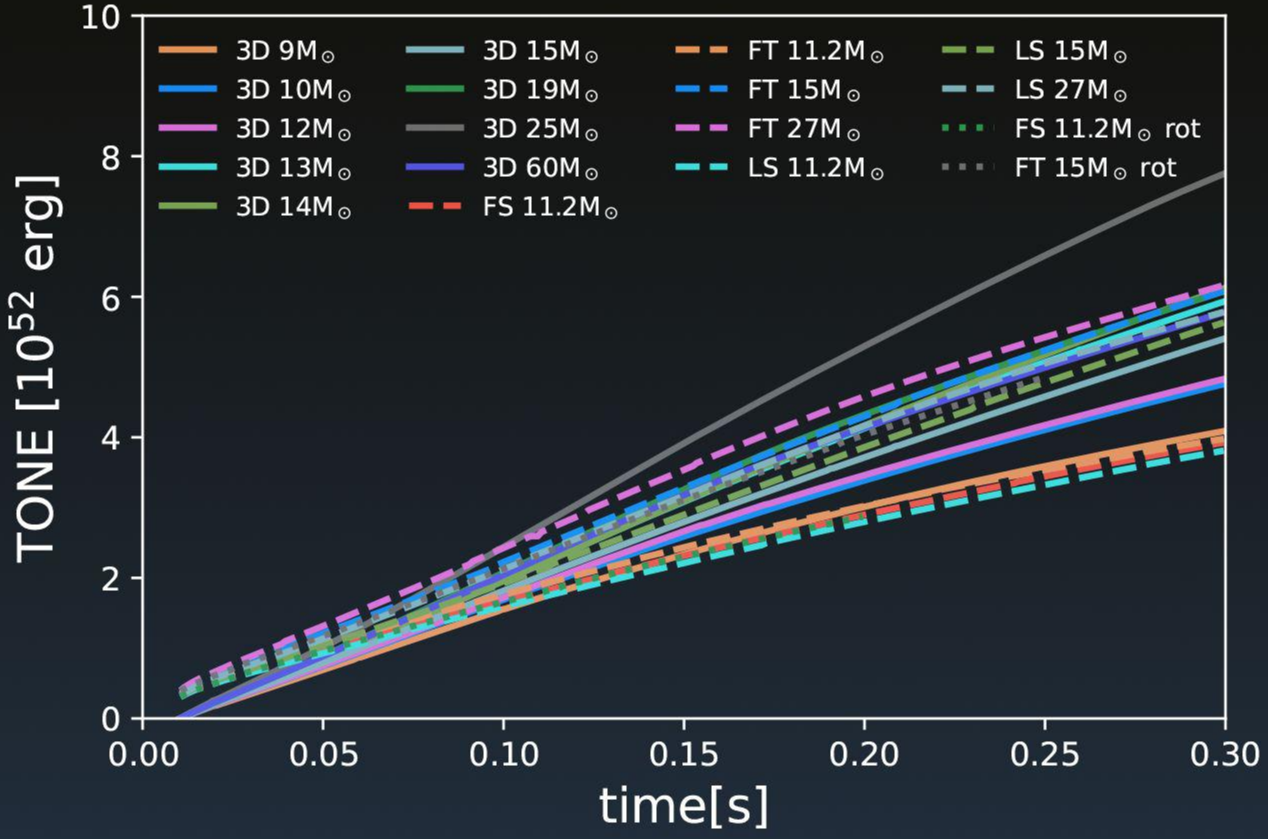

TONE [10^{52} erg]
time[s]
0
2
4
6
8
10
0.00
0.05
0.10
0.15
0.20
0.25
0.30
3D 9M$_\odot$
3D 10M$_\odot$
3D 12M$_\odot$
3D 13M$_\odot$
3D 14M$_\odot$
3D 15M$_\odot$
3D 19M$_\odot$
3D 25M$_\odot$
3D 60M$_\odot$
FS 11.2M$_\odot$
FT 11.2M$_\odot$
FT 15M$_\odot$
FT 27M$_\odot$
LS 11.2M$_\odot$
LS 15M$_\odot$
LS 27M$_\odot$
FS 11.2M$_\odot$ rot
FT 15M$_\odot$ rot

Motivation

- Various current and next-generation neutrino detection collaborations have assessed the capabilities of their detectors in observing SN neutrinos [Wang et al. 2021, Abi et al. 2021, Abe et al. 2018].
- These collaborations typically utilize a limited number (one or two) of SN models as benchmarks
- The neutrino oscillations effects and smearing effects are not always included
- Not too much analysis has been conducted to date that demonstrates the level of discrimination achievable between different SN models using several realistic detectors and interaction channels. Notable contributions in this direction: [Olsen & Qian 2022] and [Abe et al. 2021].

Conducting a study that takes into account both detector efficiencies, smearing, thresholds, background considerations, and moreover, doesn't solely focus on a limited set of benchmark models, but rather conducts a more generalized study, is a challenging task. But, it is necessary to comprehensively explore the diverse features observed in modern computer simulations.

Core-Collapse Supernovae

- Final evolutionary stage of stars with masses $M > 8\,M_\odot$. Represent a long-awaited observation target for neutrino telescopes.
- About 1% of the gravitational binding energy is released as kinetic energy in the compact object formation, while the remaining 99% is carried out by neutrinos with energies of several MeV.
- To explain these events, interdisciplinary research that combines nuclear physics, particle physics and astrophysics is needed.
- The mechanisms leading to neutrino production in the SN core are, mainly, electron capture by nucleons, pair annihilation, flavor-conversion, and nucleon bremsstrahlung:

$$e^- + p \to n + \nu_e, \quad e^+ + e^- \to \nu_e + \bar{\nu}_e, \quad \nu_e + \bar{\nu}_e \to \nu_{\tau,\mu} + \bar{\nu}_{\tau,\mu}, \quad N + N \to N' + N' + \nu + \bar{\nu}$$

- Studying the signals that the neutrino leave in the detectors, with an effective neutrino flavor discrimination, it is possible to infer properties on their physics, since the structure of the neutrino mass spectrum and lepton mixing is imprinted into the detected signal.
- CCSN neutrinos were already observed for the 1987A SN in the Large Magellanic Cloud (Kamiokande-II, Irvine-Michigan Brookhaven (IMB) an Baksan detectors)
- At present, several detectors are ready and waiting for the detection of SN neutrinos from the next galactic explosion. SN neutrinos can be detected via weak charged-current (CC) and neutral-current (NC) interactions with electrons and nuclei.
- Relevant interaction channels for current (and future) detectors: inverse beta decay, neutrino-proton elastic scattering, neutrino-electron elastic scattering, absorption interaction in liquid Argon, among others.